7

Fault Diagnosis of Induction Motors Based on FFT

Castelli Marcelo, Juan Pablo Fossatti and José Ignacio Terra
Universidad de Montevideo
Uruguay

1. Introduction

The FFT (Fast Fourier Transform) can be used for on-line failure detection of asynchronous motors. In this work a methodology is described for the most likely to happen faults in induction motors: broken rotor bars, bearing damage, short circuits and eccentricity.

In industrialized countries, induction motors are responsible for the 40% to 50% of energy consumption. The electric motors in most cases are responsible for the proper functioning of the productive system. In this line, the corrective maintenance of equipment is very expensive since it involves unscheduled downtime and damage to the production process caused by equipment failures.

Nowadays, there are many published techniques and allowed commercial tools for the induction motors failure detection. Despite this, most industries still do not use detection and monitoring techniques of electrical machines.

Here a methodology for monitoring and diagnosis of induction motors is presented, which monitors the engine without removing it from the production line, being this methodology: reliable, easy to apply and low cost.

Next a brief study of the most likely faults to occur in induction motors has been made, as well as the existing methods for detecting them.

Then, a methodology based on the measurement of the stator current signal has been developed. This can show the frequency and magnitude of each failure happen to occur in this kind of engines.

After that, the methodology has been carried out to validate in the laboratory.

2. Failures in induction motors

Most failures in induction motors can be classified in two main groups: isolation failures and mechanical failures (Botha, 1997).

Isolation failures are commonly characterized by stator coils short-circuits, while mechanical faults are commonly associated to rotor or rotor related damage. The most important mechanical failures are: rotor broken bars and rings, bearings damage, irregular gaps (static and dynamics eccentricities), unbalances, refrigeration troubles, etc.

In general, faults in electrical machines are dominated by failures in bearings and stator coils. Focused on asynchronous motors with squirrel cage rotor failure statistics are the following (Fig. 1) (Thomson & Fenger, 2001):

- Bearings fault related: 41%
- Stator faults related: 37%
- Rotor faults related: 10:
- Other problems: 12%

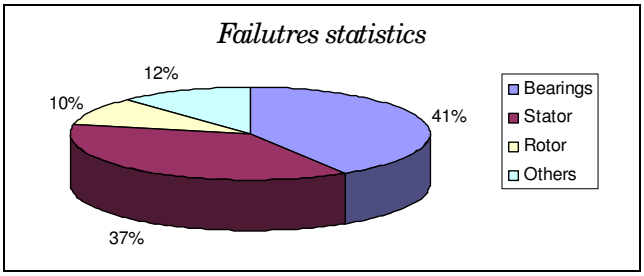

Fig. 1. Failures statistics in induction motors

The previous analysis of the most likely to happen failures in asynchronous motors showed the tree types that represent the 90% of the possible failures in those motors. Being the punctual failures:

- Bearing fault related
- Rotor broken bars and rings.
- Stator coils short-circuits
- Stator unbalance and eccentricities

2.1 MCSA (Motor Current Signature Analysis)

The main objective of the developed methodology is the motor slip determination using only the stator current. This parameter could be used for many applications, but this work is focused on fault detection via MCSA (Motor Current Signature Alalysis).

The on-line diagnosis via MCSA is used to detect several faults such as: stator and rotor failure, bearing damage and eccentricities in induction motors (Thomson, 1999) (Thomson & Gilmore, 2003). This method is based on the fact that an unbalanced machine when supplied with a three phase balanced voltage produces specific components in the stator current, whose magnitude and frequency depends on the asymmetry level and nature of the fault (Bellini et al, 2002). This method is based on the current signal spectrum decomposition, analyzed via the Fast Fourier Transform. The fault causes a harmonic component in the current at a characteristic frequency, visualized in the current spectrum. To determine these frequencies the motor slip should be known.

2.2 Eccentricity

There are two types of air gap eccentricity: the static air gap eccentricity and the dynamic air gap eccentricity. In the case of the static air gap eccentricity, the position of minimal radial

air-gap length is fixed in space. Thus for example, static eccentricity can be caused by the ovality of the core or by the incorrect positioning of the stator or rotor at the commissioning stage. In the case of the dynamic eccentricity the center of the rotor is not at the center of rotation and the position of the minimum air-gap rotates with the rotor. For example, dynamic eccentricity can be caused by a bent rotor shaft, wear of bearings, misalignment of bearings, mechanical resonances al critical speed and so on.

The frequency components in the stator current of an induction machine which are due to air gap eccentricity can be obtained as:

$$f_{ec} = f_1 \pm k.f_{rm} \tag{1}$$

Where,
f_{ec} = eccenticity frequency
f_1 = supply frequency
f_{rm} = rotor mechanical frequency
k = 1, 2, 3….

2.3 Slip estimation methodology

Here a slip estimation methodology using the frequency stator current spectrum is presented. The main objective is to identify the eccentricity associated component and therefore obtain the rotor speed.

First, the motor nominal speed must be known in order to determine the frequency range in which the eccentricity component can be found. Then, from (ec1) the fault associated frequency is calculated for nominal rotor speed.

$$f_{ecn} = f_1 \pm f_{rmn} \tag{2}$$

Where,
f_{ecn} = eccentricity frequency (at motor nominal speed)
f_1 = supply frequency
f_{rmn} = rotor nominal mechanical frequency

It is important to say that $k = \pm 1$ because the range in which the eccentricity frequency can be found is reduced to the maximum.

After the motor's nominal eccentricity frequency calculation, the motor current is determined, in order to specify if the eccentricity frequency (f_{ec}) is lower o higher than the nominal eccentricity frequency (f_{ecn}). For example, if we take $k = -1$ and the motor current is higher, then the eccentricity frequency is lower than the nominal eccentricity frequency. Table 1 shows the relationship between intensity, eccentricity frequency and rotor mechanical frequency and their nominal values. Where I is the measured current and I_N the nominal current.

Then, to bound the range of values where the eccentricity associated component can be found, reasonable limits for the motor speed have been established. For example, a motor with two pairs of poles and a measured current higher than the nominal, whose maximum rotor mechanical frequency is 25 Hz. Working with k=-1 it is possible to establish a minimum limit for the eccentricity frequency.

$$f_{ec}(\min) = f_1 - f_{rm}(\max) \tag{3}$$

$k=1$		$k=-1$	
$I > I_N$	$I \le I_N$	$I > I_N$	$I \le I_N$
$f_{ec} < f_{ecn}$	$f_{ec} \ge f_{ecn}$	$f_{ec} > f_{ecn}$	$f_{ec} \le f_{ecn}$
$f_{rm} > f_{rmn}$	$f_{rm} \le f_{rmn}$	$f_{rm} < f_{rmn}$	$f_{rm} \ge f_{rmn}$

Table 1. Relationship between intensity, eccentricity frequency and rotor mechanical frequency

Then, the eccentricity frequency is bounded as follows:

$$f_{ec}(\min) \le f_{ec} \le f_{ecn} \tag{4}$$

If the nominal speed is 1435 rpm and the supply frequency is 50 Hz, the eccentricity frequency will be in a 1.08 Hz wide window.

$$25Hz. \le f_{ec} \le 26.08Hz. \tag{5}$$

If the stator current is higher than the nominal ($f_{rm} < f_{rmn}$), for setting a maximum limit for the eccentricity frequency a minimum rotor speed should be set. In this work the maximum slip limit was taken as 5 %, other slip values could be considered depending on the case.

$$f_{ecn} < f_{ec} \le f_{ec}(\max) \tag{6}$$

Where $f_{ec}(\max)$ calculation is based on considering a maximum slip of 5%. For example if we consider a motor with two pairs of poles with nominal speed of 1435 rpm and supply frequency of 50 Hz, the eccentricity frequency is bounded as follows:

$$26.08Hz < f_{ec} \le 26.25Hz \tag{7}$$

The eccentricity frequency can be found in a 0.17 Hz window, this allows an almost immediate identification. For the motor tested the sampling time was 8 seconds, thus a 0.125 Hz resolution. This makes possible an accurate identification of the eccentricity component and little motor speed variation.

Another important thing is that there is no mask effect, since the eccentricity frequency is far enough from the supply frequency associated component.

Once the eccentricity associated component is calculated, its associated frequency has to be determined. Being a_k the kth harmonic associated to the discrete Fourier Transform (DFT) and tm the sampling time, the eccentricity frequency is determined as follows:

$$f_{ec} = \frac{k \pm \frac{1}{1+\Psi}}{tm} \tag{8}$$

Where,

$$\Psi = \frac{|a_k|}{Max(|a_{k+1}|,|a_{k-1}|)} \tag{9}$$

Being a_k the main harmonic associated with the eccentricity frequency. It is important to say that ec8 is valid when there are no other components due to different causes next to the interest component, and that no temporary windows are used.

Finally, once the eccentricity associated frequency is found, it is possible to find from ec1 the rotor mechanical frequency and so, the slip.

2.4 Data acquisition model

There are several techniques that can be used for detecting faults in induction motors. The MCSA (Motor Current Signal Analysis) is a non-invasive, on-line monitoring technique for diagnosing problems in induction motors. This method is based on the spectral decomposition of the steady state stator current which can be acquired with simple measurement equipment and under normal operation of the machine. MCSA can diagnose problems such as broken rotor bars, shorted turns, bearing damage and air gap eccentricity. In the MCSA method the current frequency spectrum is obtained and analyzed aiming to find out specific components which can indicate an incipient fault in the machine. These frequencies are related to well-known machine faults. Therefore, after the processing of the stator current, it is possible to infer about the machine's condition.

A methodology with an accurate comprehension of the different influence of the variables is desired for the correct interpretation of the data acquired. In this work the frequency spectrum is obtained by the fast Fourier transform (FFT). For the case that the data acquisition is for a entire number of cycles of a certain component is easy to obtain its amplitude and frequency, this is not always the case. In consequence we will have in the frequency spectrum certain components that could mask others of interest. This is commonly known as leakage. Another thing to take into account is the fact that the motor's load condition is not always the same; this makes the fault signature characteristics different. The main objective of this methodology is to monitor these frequencies independently of the motor functioning and the data acquisition in order to determine the condition of the machine. To avoid the masking effect, the signal is multiplied by a function (window) reducing the discontinuity. In this opportunity we are not going to analyze the use of the different windows, but we focus in the acquisition of the signal's amplitude introduced by the failure.

2.5 Monitoring and diagnosis methodology

Here the fault frequency equations for the measured current signal deduced via the analysis of Fast Fourier Transform for each defect are presented.

2.5.1 Broken bars

For the case of broken rotor bars the equation is the following:

$$f_b = f_1(1 \pm 2s) \tag{14}$$

Where,

f_b = broken bars frequency
f_1 = supply frequency
s = slip frequency

2.5.2 Short-circuits

For short-circuits in induction motors:

$$f_{st} = f_s.\left\{\frac{n}{p}.(1-s) \pm k\right\} \tag{15}$$

Where,
f_{st} = short-circuit frequency
f_s = supply frequency
n = 1, 2, 3…
p = pole pairs
s = slip frequency
k = 1, 3, 5…

2.5.3 Eccentricities

For the eccentricities, the equation is the following:

$$f_{ec} = f_s.\left[(r \pm n_d).\left(\frac{1-s}{p}\right) \pm n_{ws}\right] \tag{16}$$

Where,
f_{ec} = eccentricity frequency
f_s = supply frequency
r = number of slots
n_d = +/− 1
p = pole pairs
s = slip frequency
n_{ws} = 1, 3, 5…

2.5.4 Bearing failures

Finally the equation for bearing failure:

$$\begin{aligned} f_0 &= 0.4 * n * f_{rm} \\ f_1 &= 0.6 * n * f_{rm} \end{aligned} \tag{17}$$

Where,
f_0 = lower frequency
f_1 = upper frequency
n = balls number
f_{rm} = rotor mechanical frequency

The equation 17 applies only when cyclic faults occur and only for bearings between 6 and 9 balls.

It is necessary to know the motor's simplified equivalent circuit to study. Based on the simplified equivalent circuit, and doing current and voltage measurement, it is possible to find the slip motor. It should be borne in mind that the slip found in this way is very sensitive to small variations of the parameters calculated before. Therefore the realization of an FFT of the current signal is necessary, as the harmonics of eccentricity of the motor are always present in this spectrum and this harmonics give us, from the applications of equations: 12 and 13, an accurate measure of the fault frequency, which form equation 18 provides a very precise measurement of slip frequency, which is used to identify all the failure frequencies.

$$f_{ec} = f_s \pm k \cdot f_{rm} \tag{18}$$

Where
f_{ec} = eccentricity frequency
f_s = supply frequency
k = 1, 2, 3…
f_{rm} = rotor mechanical frequency

From the current sampling and the slip frequency of the motor, it is possible to determine the frequencies for each failure study.

It is necessary to remark the fact that in the data acquisition, the FFT of the measured current was normalized as a function of the primary harmonic amplitude, in order to obtain fault amplitude independent form the motor load condition.

After determining the true amplitudes and frequencies of defect, it is necessary to study its evolution in time, for the selected motors.

2.6 Exact amplitude and frequency determination

Here the mathematical development in order to determine the exact amplitude and frequency of the failure.

First a brief description of the signal current reconstruction is shown. Then, a mathematical development is presented based on an accurate sampling of N periods of the signal current. After that the problems due to sampling of no-exact number of cycles are shown, and later the mathematical development that eliminates that problem.

$X[n]$	Discrete Fourier Transform
$x[n]$	Discrete function
N	Number of total samples
T	Time period
t	Time
$n = 0, \pm1, \pm2, ...$	
$k = 0, \pm1, \pm2, ...$	
ω_0	Fundamental frequency (for discrete and continuous)
a_k	Spectral coefficient (for discrete and continuous)
t_m	Sampling time
ω_s	Sampling frequency
ω_m	Minimum Sampling frequency

$\bar{x}$ Data vector
$\bar{X}$ Data vector ($\bar{X} = FFT(\bar{x})$)
$x(t)$ Signal as a function of time
j Imaginary unit
Ψ $\Psi = \frac{|a_k|}{|a_{k\pm1}|}$ relationship between the main harmonic and the one that follows in amplitude
y Real value that indicates the number of cycles sampled above or below (depending on their sign) of the k cycles when evaluation the k-th harmonic
y' Real value that indicates the number of cycles sampled above or below (depending on their sign) of the k cycles when evaluation the k-th harmonic, being the last the main harmonic.
T Period of a function

2.7 Signal reconstruction

One of the most important issues to take into account for the proper failure detection is the signal interpretation. The signal is composed of sinusoidal continuous waves at different frequencies. These components will be in part caused by different defects that may exist and the characteristics of the load. Another aspect to consider is that the methodology should be versatile to adapt to different working conditions.

From the stator current sampling the different frequencies that and the wave amplitudes should be obtained. Then with these parameters the failure (the frequency) and its importance (amplitude) is obtained.

To reconstruct the original signal, among other things, the Fast Fourier Transform (FFT) will be used. The FFT is an algorithm that can efficiently calculate the discrete Fourier transform (DFT). This algorithm was created in 1965 by JW Cooley and JW Tuckey

The direct calculation of the DFT involves a number of operations proportional to N^2 (where N is the number of samples) while using the fast Fourier transform the number of operations is proportional to $NLog_2(N)$. This markedly reduces the calculating time of the discrete Fourier transformed. This last fact combined with the increased processing power of computers made the FFT become a fundamental tool in many disciplines. Communications, signal processing, sonar, radar, biomedical engineering, inventory analysis, metallurgy and applied mechanics are just some of the areas where the FFT is applied.

Note that to properly apply the fast Fourier transform is not necessary to have a thorough knowledge of the algorithm. Instead it is important to understand the discrete Fourier transform and therefore the Fourier transform.

2.8 Mathematical development

The following is an introduction to Fourier series representation of discrete periodic signals and discrete Fourier transform (DFT). Similar to continuous functions, the fundamental period N is defined and the fundamental frequency ω_0 , such that: $x[n] = x[n+N]$

where N is the smallest integer that fulfills the above relationship.

$$\omega_0 = \frac{2\pi}{N} \tag{19}$$

Then $\theta_k[n]$, that we define as:

$$\theta_k[n] = e^{j\omega_0 kn} = e^{j\frac{2\pi}{N}kn} \tag{20}$$

With k = p, p+1,…, (N-1) + p (with p integer) or $k = \langle N \rangle$

then $\theta_k[n] = \theta_{k+rN}[n]$ (with r integer).

As follows $x[n]$ as a combination of complex exponentials:

$$x[n] = \sum_{k=\langle N \rangle} a_k \theta_k[n] = \sum_{k=\langle N \rangle} a_k e^{j\omega_0 kn} = \sum_{k=\langle N \rangle} a_k e^{j\frac{2\pi}{N}kn} \tag{21}$$

Where a_k can be expressed:

$$a_k = \frac{1}{N} \sum_{n=\langle N \rangle} x[n] e^{-j\omega_0 kn} \tag{22}$$

With $a_k = a_{k+N}$ and $a_k = \overline{a_{-k}}$ (only when $x[n]$ is real for all n).

In a similar way the Discrete Fourier Transform (DFT)is defined as:

$$x[k] = \sum_{n=\langle N \rangle} x[n] e^{-j\frac{2\pi}{N}nk} = \sum_{n=\langle N \rangle} x[n] e^{-j\omega_0 nk} \tag{23}$$

The inverse Discrete Fourier Transform (IDFT) can be expressed as follows:

$$x[n] = \frac{1}{N} \sum_{k=\langle N \rangle} X[k] e^{j\frac{2\pi}{N}nk} = \frac{1}{N} \sum_{k=\langle N \rangle} X[k] e^{j\omega_0 nk} \tag{24}$$

With the algorithm FTTW, Matlab obtains the DFT from a data vector composed:

$$\bar{x} = [x[0], x[1], \ldots, x[N-1]] \tag{25}$$

Is the same as: $\bar{x}(n) = x[n-1]$

When doing the FFT($\bar{x}$) an $\overline{X}$ vector is obtained given by the following expression:

$$X(k) = \sum_{i=1}^{N} x(i) \omega_n^{(i-1)(k-1)} \tag{26}$$

With $\omega_n = e^{-\frac{2\pi}{N}j} = e^{-\omega_0 j}$

The k-th value of the $\overline{X}$ vector corresponds to (k-1)t harmonic:

$$\overline{X}(k) = X[k-1] = a_{k-1}N \tag{27}$$

Or,

$$\overline{X}(k) = [a_0, a_1, ..., a_{N-1}]N \tag{28}$$

In order to know the reach of the DFT and make a correct interpretation some examples are shown:

Figure 2 shows the sampling of a sinusoidal signal of amplitude 1.

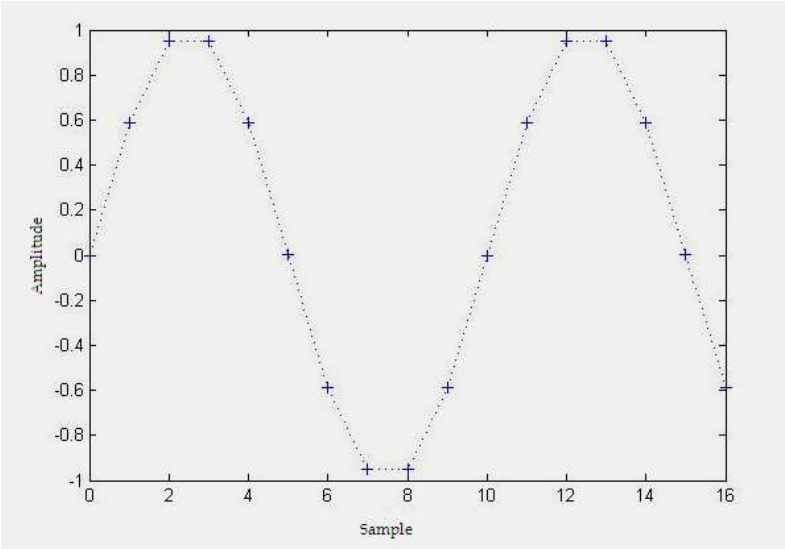

Fig. 2. Sinusoidal signal

If N=10 and the samples were taken during one period:

$$\bar{x} = [\sin(\frac{2\pi}{10}0), \sin(\frac{2\pi}{10}1), \sin(\frac{2\pi}{10}2), ..., \sin(\frac{2\pi}{10}9)] \tag{29}$$

It is possible to express $x[n]$ as follows:

$$x[n] = \frac{1}{2j}e^{j\frac{2\pi}{10}n} - \frac{1}{2j}e^{-j\frac{2\pi}{10}n} \tag{30}$$

Which is the same as:

$$x[n] = \frac{1}{2j}e^{j\frac{2\pi}{10}n} - \frac{1}{2j}e^{j\frac{2\pi}{10}9n} \tag{31}$$

By doing the FFT $\bar{x}$ an $\bar{X}$ vector is obtained, where:

$$\bar{X}(2) = X[1] = Na_1 = \frac{N}{2j} \tag{32}$$

$$\bar{X}(9) = X[9] = Na_9 = -\frac{N}{2j} \tag{33}$$

For the other positions: $\bar{X}(i) = 0$.

Supposing 10 samples of the same function with a phase shift: $\theta = \frac{2\pi}{10}3$.

The following data vector $\bar{x}$ is obtained

$$\bar{x} = [\sin(\frac{2\pi}{10}3), \sin(\frac{2\pi}{10}4), \sin(\frac{2\pi}{10}5), ..., \sin(\frac{2\pi}{10}12)] \tag{34}$$

$$x[0] = \sin(\frac{2\pi}{10}3), x[1] = \sin(\frac{2\pi}{10}4), \ldots, x[9] = \sin(\frac{2\pi}{10}12)$$

Then, it is possible to express $x[n]$ as follows:

$$x[n] = \frac{1}{2j}e^{j(\frac{2\pi}{10}n + \frac{2\pi}{10}3)} - \frac{1}{2j}e^{-j(\frac{2\pi}{10}n + \frac{2\pi}{10}3)} \tag{35}$$

Then:

$$\bar{X}(2) = X[1] = \frac{N}{2j}e^{j\frac{2\pi}{10}3} \tag{36}$$

$$\bar{X}(10) = X[9] = -\frac{N}{2j}e^{-j\frac{2\pi}{10}3} \tag{37}$$

To generalize, the DFT is analyzed for N samples of a sinusoidal function period with β amplitude and $\theta = \frac{2\pi}{N}d$ phase shift, with $d = 0, \pm 1, \pm 2...$ or $x[n] = \beta \sin(\frac{2\pi}{N}n + \frac{2\pi}{N}d)$. The following vector is obtained $\bar{X}$:

$$\bar{X}(2) = X[1] = \frac{\beta N}{2j}e^{j\frac{2\pi}{N}d} \tag{38}$$

$$\bar{X}(N) = X[N-1] = -\frac{\beta N}{2j}e^{-j\frac{2\pi}{N}d} \tag{39}$$

The wave amplitude is given by:

$$|X(2)|\frac{2}{N}=|X[1]|\frac{2}{N}=\beta \tag{40}$$

Taking N samples during two periods.

$$\begin{aligned} x[n] &= \beta\sin(2\frac{2\pi}{N}n+2\frac{2\pi}{N}d) \\ &= \frac{\beta N}{j2}e^{j\frac{2\pi}{N}2d}e^{j\frac{2\pi}{N}2n}-\frac{\beta N}{j2}e^{-j\frac{2\pi}{N}2d}e^{-j\frac{2\pi}{N}2n} \\ &= \frac{\beta N}{j2}e^{j\omega_0 2d}e^{j\omega_0 2n}-\frac{\beta N}{j2}e^{-j\omega_0 2d}e^{-j\omega_0 2n} \end{aligned} \tag{41}$$

For the generic case where k periods are sampled of a sinusoidal function of β amplitude and phase shift $\theta=\frac{2\pi}{N}d$, it is possible to express $x[n]$ as follows:

$$x[n]=\frac{\beta N}{j2}e^{j\omega_0 kd}e^{j\omega_0 kn}-\frac{\beta N}{j2}e^{-j\omega_0 kd}e^{-j\omega_0 kn} \tag{42}$$

So:

$$a_k=\frac{\beta N}{j2}e^{j\omega_0 kd} \text{ y } a_{N-k}=a_{-k}=-\frac{\beta N}{j2}e^{-j\omega_0 kd}$$

Therefore, if a vector is generated $\bar{x}$ = [$x[0],x[1],...x[N-1]$] then the FFT $\bar{X}=FFT(\bar{x})$ is as follows:

$$\bar{X}(k+1)=X[k]=a_k \tag{43}$$

$$\bar{X}(N-k+1)=X[n-k]=a_{N-k}=a_{-k} \tag{44}$$

For the rest of the values: $\bar{X}(i)=0$

If N samples of k periods for any sinusoidal function would be easy to find the original signal amplitude as shown by the following equation:

$$\beta=|\bar{X}(k+1)|\frac{2}{N}=|\bar{X}[n]|\frac{2}{N} \tag{45}$$

Being tm the sampling time, assuming complete cycles, then it is possible to deduce the exact frequency (f) and the amplitude.

$$f=\frac{k}{tm} \tag{46}$$

3. Laboratory tests results

In this section, laboratory tests results for: broken rotor bars, short-circuit, eccentricities and bearing failure are presented.

3.1 Broken rotor bars

The broken rotor bar simulation was achieved by perforation in the bars with a drill (Figure 3).

Fig. 3. Rotor perforations

First the tests were carried out with the healthy motor. Then the rotor was perforated in order to simulate the broken rotor bars failure (Fig. 4).

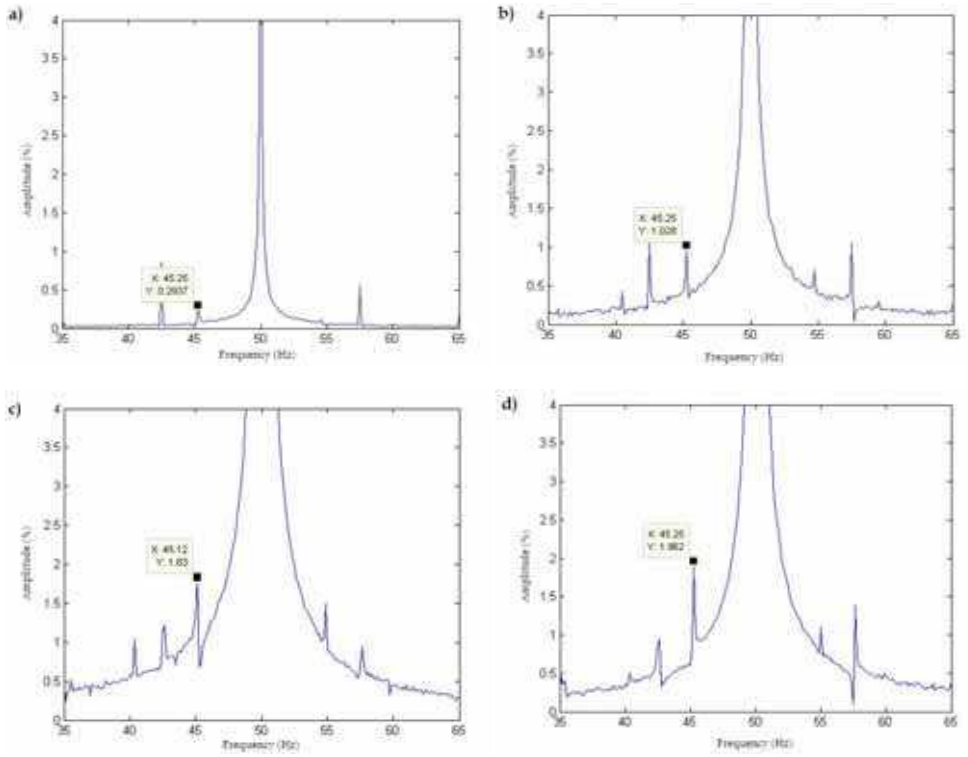

Fig. 4. a) Healthy motor; b) One broken bar; c) Two broken bars; d) Three broken bars

For all the test the amplitude was normalized to the main harmonic and the test were carried out with a constant charge (1429 rpm).

The frecuencies where should appear the failure components:

Revolutions: 1429 rpm

$$s = \frac{1500 - 1429}{1500} = \ 0.0473$$

$$fc = f \cdot (1 \pm 2.s)$$

$$fc^{+} = 54.7300 \text{ HZ}$$

$$fc^{-} = \ 45.2700 \text{ HZ}$$

For all of the cases the presence of the harmonics on that frequency can be verified. Also it is important to say that there is a clear relationship between the number of broken bars and the relative amplitude of the harmonics (Table 2) (Figure 5). It should be noted that in rotor broken bars failure, cancelation occurs if they have a phase shift of 180 electrical degrees between two broken bars.

Frequency (Hz)	Amplitude (%)	Number of broken bars
45.25	0,294	0
45.25	1,028	1
45.25	1,830	2
45.25	1,962	3

Table 2. Relative Amplitude for the different number of broken bars tested

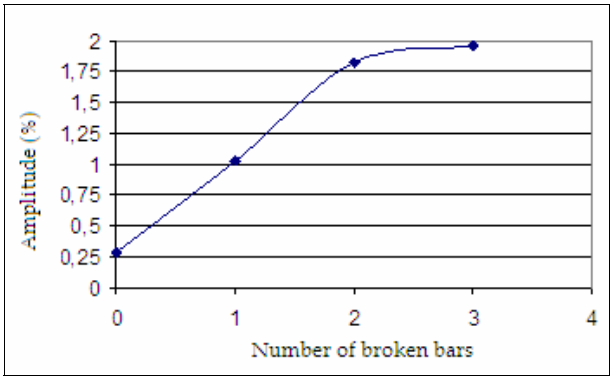

Fig. 5. Failure evolution (Amplitude vs. Number of broken bars)

As seen in Fig. 6 there is no appreciable difference between with one broken bar and five broken bars. This is due to the fact that there is electrical symmetry between 2 pairs of them. This reflects a limitation of the proposed methodology in terms of diagnostic capability of damage if they occur symmetrically.

This methodology not only detects the presence of a defect but also makes it possible to establish a trend. It is important for determining whether the engine should continue to operate or if necessary out of service (the latter is essential). On the other hand, is that the presence of symmetrical defects could be a drawback to detect broken bars. Finally, it is possible to use this type of industrial-level diagnosis for the detection of broken bars in induction motors.

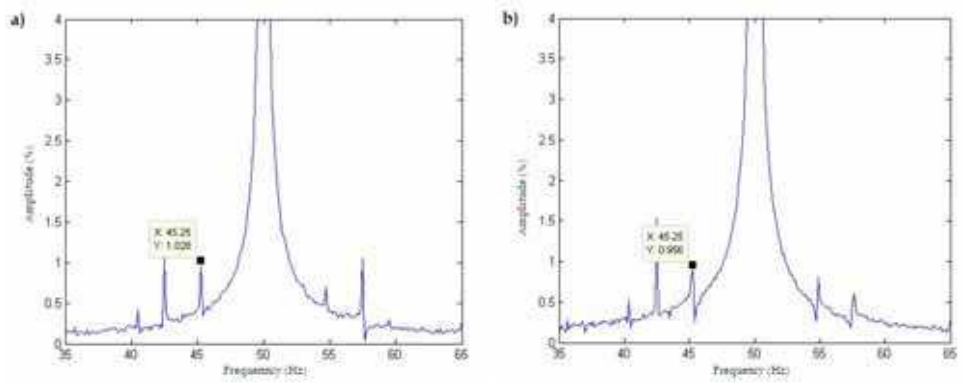

Fig. 6. a) One broken bar; b) Five broken bars

It must be said that cyclical loads can produce frequency responses similar to broken bar failures.

3.2 Short-circuit

Of all the types of short-circuit that can occur in the engine (Fig. 7), the ones that occur at the same stage are more difficult to detect (this is due to the fact that the protections are not activated). This is why the work focuses on this type of failure.

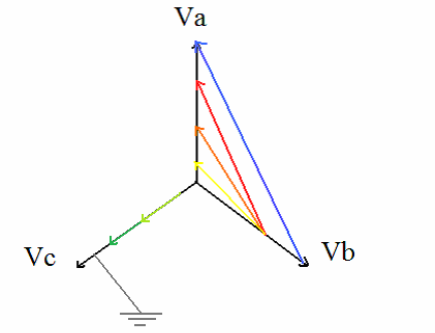

Fig. 7. Different types of short-circuit. In blue, orange, yellow and red the short-circuits are between two phases of different magnitudes. In gray a ground fault is represented and in green two shorts of the same phase of different magnitudes (these defects are the ones that will be simulated)

The potential difference was measured between the different points in order to determine the short-circuit magnitude. The result is shown in Table 3 which expresses the potential difference and the percentage that this represents. Fig. 8 shows how each cable was connected and then smoothed through a hole to simulate a short circuit.

Fig. 8. Induced short-circuit

	1	2	3	4	5	6	7
1							
2			0.51	1.58	0.64	5.81	1.93
3		1.95%		1.15	0.11	6.34	1.39
4		6.05%	4.41%		1.02	7.51	0.22
5		2.45%	0.42%	3.91%		6.47	1.27
6		22.26%	24.29%	28.77%	24.79%		7.75
7		7.40%	5.33%	.84%	4.87%	29.69%	

Table 3. Short-circuit magnitude

The tests were carried out for short-circuits of: 0% (healthy motor), 1.02%, 1.39% and 1.95%% (Fig. 9) at 1477rpm (s=0.015). For these work conditions the characteristically frequency for short-circuit 23.85 Hz (with n=3 y k=1).

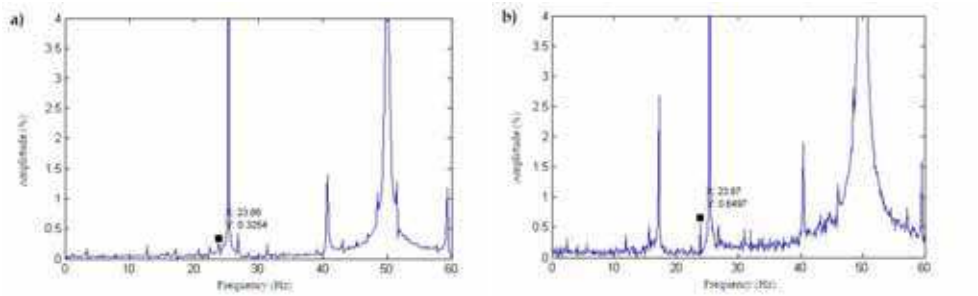

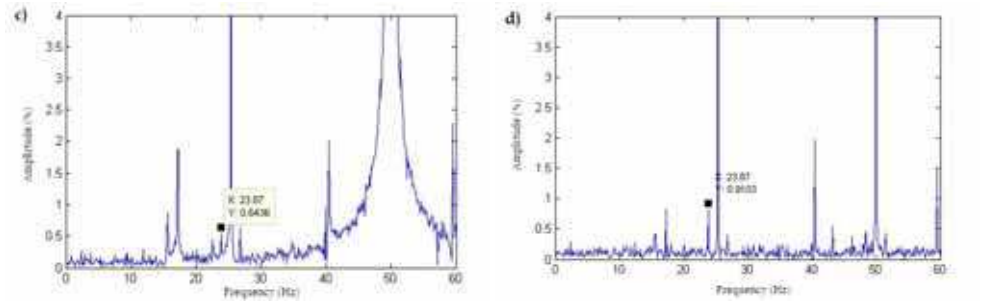

Fig. 9. a) Healthy motor; b) Short-circuit of 1.02 %; c) Short-circuit of 1.39 %; d) Short-circuit of 1.95 %

Frequency (Hz)	Amplitude (%)	Short-circuit (%)
23.84	0.80	0
23.84	1.34	1.02
23.85	1.47	1.39
23.85	1.89	1.95

Table 4. Amplitude for the different short-circuit magnitude

In table 4 the different short-circuits tested. The presence of a harmonic at a frequency of 23.84Hz coincides with the previous slip s measurement (23.85 Hz). Then, the short-cut magnitude (at 25.36 Hz) as a function of the defect amplitude (Fig. 10).

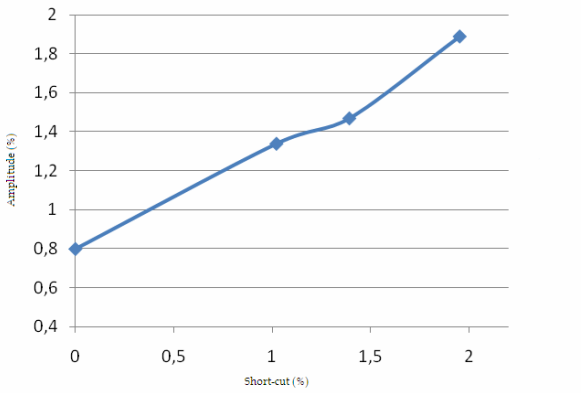

Fig. 10. Amplitude vs. short-cut magnitude

It can be concluded that there is a strong tendency as the magnitude of the defect increases above 1.0%, (Fig. 10). It is possible to predict the existence of a short circuit that due to its magnitude has not occurred to activate the protection, but would be able to leave the engine inoperative.

In high voltage motors it is very short the time between a short circuit within a phase and a short circuit between phases (seconds or minutes). This makes this methodology difficult to implement.

3.3 Bearing failure

First the tests were carried out with the healthy motor. Then the bearings were manipulated with a punch in order to simulate the bearing damage, one at the time (Fig. 11). The sampling was carried out at 5kHz during 8 seconds. In table 5 the rotor speed for each test, where test 1 is with the healthy motor, 2, 3 and 4 correspond to 1, 2 and 4 bearing damage.

Test	Speed (rpm)	Rotor frequency (Hz)
1	1482	24.70
2	1482	24.70
3	1482	24.70
4	1483	24.72

Table 5. Rotor speed and failure frequency for each test

It is possible to obtain the related failure frequency for bearing damage. For a rotor speed of 1482 rpm, the failure frequency is: 69.15 Hz and 69.20 Hz for a speed of 1483 rpm.

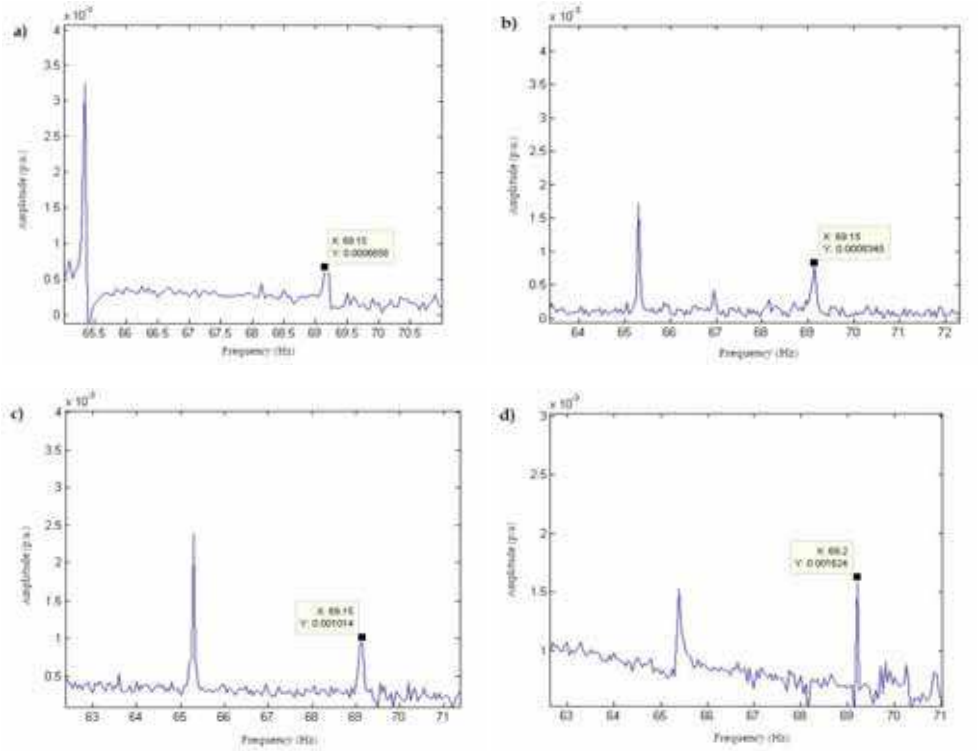

Fig. 11. a) Healthy motor; b) One bearing damage; c) Two bearings damage; d) Four bearings damage

The failure amplitude increases with the number of damaged bearings (Table 6) (Fig. 12). In Fig. 13 the damage simulated in the studied bearing.

Test	Failure Amplitude (%)
1	0.105
2	0.110
3	0.160
4	0.185

Table 6. Failure amplitude for each test

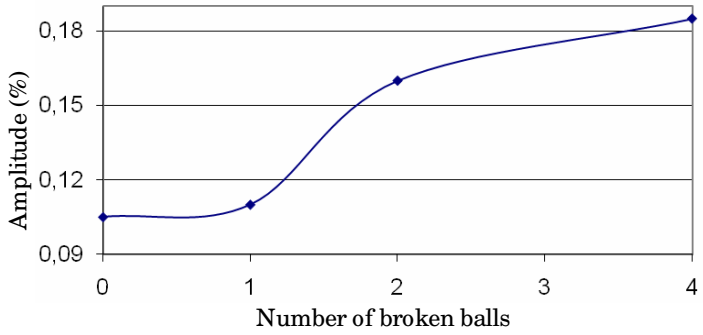

Fig. 12. Amplitude vs. number of damaged bearings

Fig. 13. Bearing damage

It is possible to detect bearing damage with the diagnostic methodology presented here. It is important to mention that none of the defects introduced into the engine in order to determine the course of the defect and the severity of the fault, have prevented the proper operation under the same load condition. Taking this into account it can be concluded that for this particular case, it is possible to detect the damage in time for scheduling preventive maintenance stop.

3.4 Eccentricities

In order to measure the eccentricity the center position of the rotor from a fixed reference was measured. Then the relative displacement of the rotor with respect to the baseline, as a percentage of nominal air gap of the machine was calculated. In Fig. 14 the eccentricity induced failure, in Fig. 15 the eccentricity generation.

Fig. 14. Eccentricity induced failure

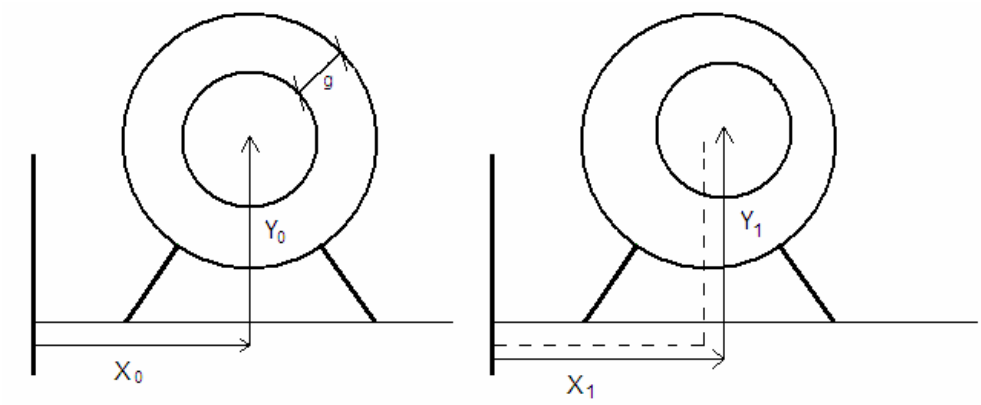

Fig. 15. Eccentricity generation

From the different measurements the eccentricity was calculated as a percentage using the following expression:

$$e(\%) = \frac{\sqrt{(x_1 - x_0)^2 + (y_1 - y_0)^2}}{g} \tag{47}$$

In table 7 the results for each test.

Test	Eccentricity (%)	speed (rpm)	Frequency (Hz)
1	0	1393	26.79
2	44,5	1400	26.67
3	87.3	1361	27.31

Table 7. Eccentricity results

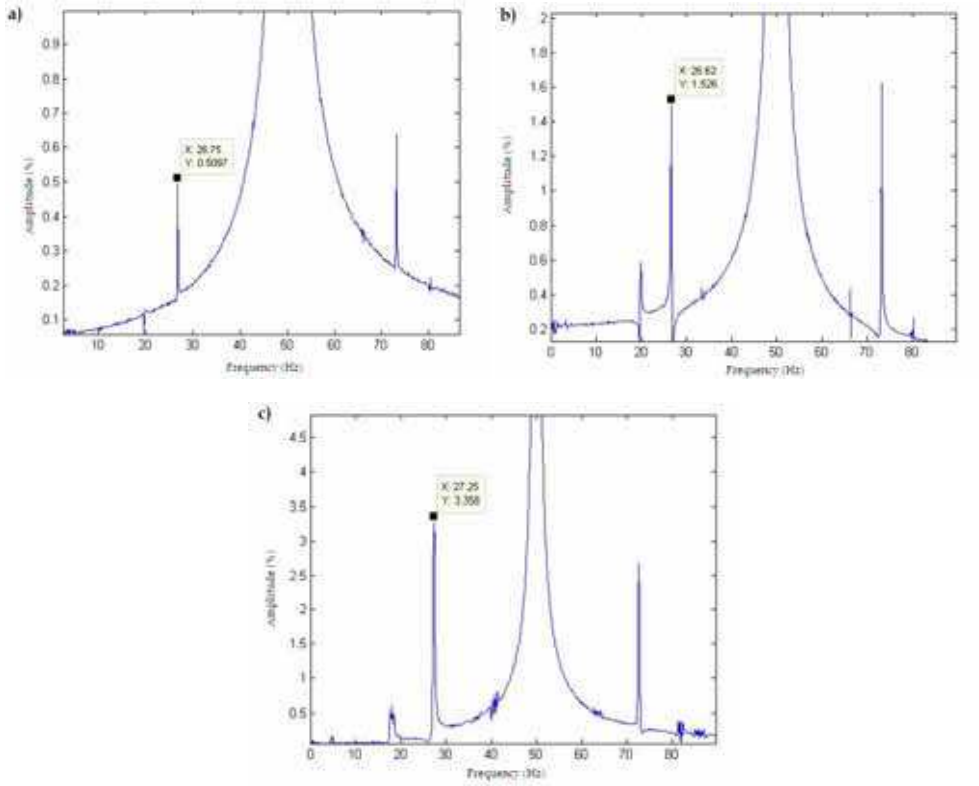

Fig. 16. a) Healthy motor; b) e=44.5%; c) e=87.3%

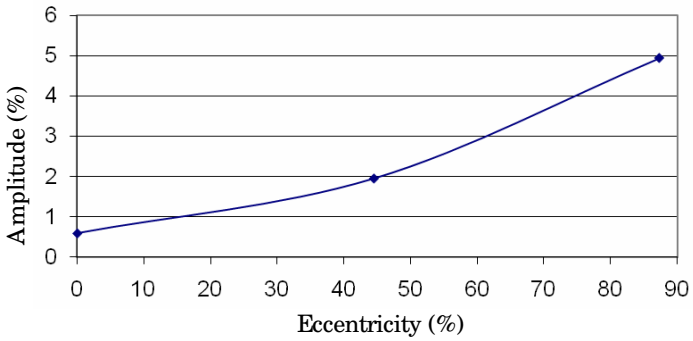

Fig. 17. Failure amplitude vs. eccentricity

There is a clear relationship between the failure amplitude and the amount of eccentricity (Table 8) (Fig. 17). In Fig. 18 the induced eccentricity failure.

The methodology proposed in this work is capable of detecting eccentricity failures and its evolution as a function of the defect amplitude. It should be noted however, that the tests

performed with the prototype built for this purpose, develop an intrinsic eccentricity defect. Thus, although the proposed methodology has been tested for the detection of this defect, at the industrial level should be monitored by studying the evolution of the defect in several tests and not from a standard that can be built from trials in the test.

Eccentricity (%)	Amplitude (%)
0	0.59
44,5	1.96
87,3	4.94

Table 8. Failure amplitude

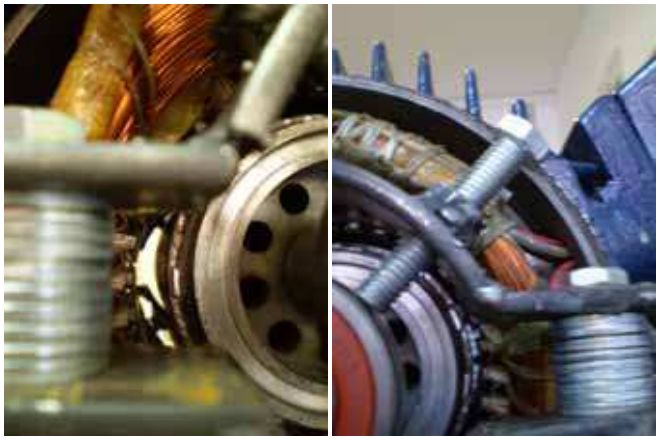

Fig. 18. Eccentricity failure

4. Industrial tests results

In this section, the results of industrial tests are presented. In table 9 the main characteristics of the motor tested (Fig. 19).

Fig. 19. Tested motor

POWER	250Hp
Number of pole pairs	3
Nominal Voltage	380V

Table 9. Main motor characteristics

The known information for the tested motor is poor. First the stator current was measured (Fig. 20). Then the normalized FFT of the sampled signal was carried out (Fig. 21).

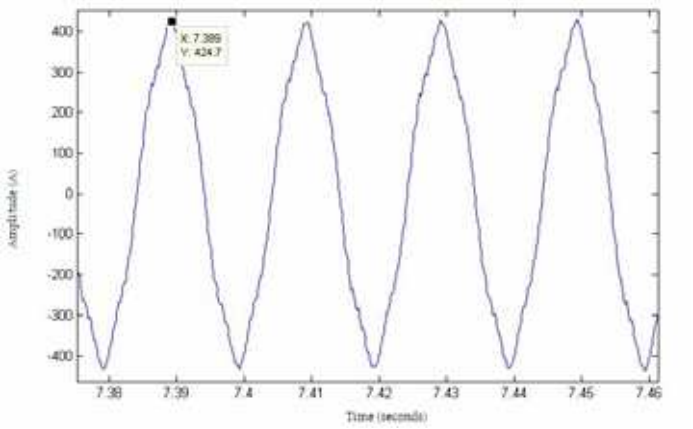

Fig. 20. Stator current

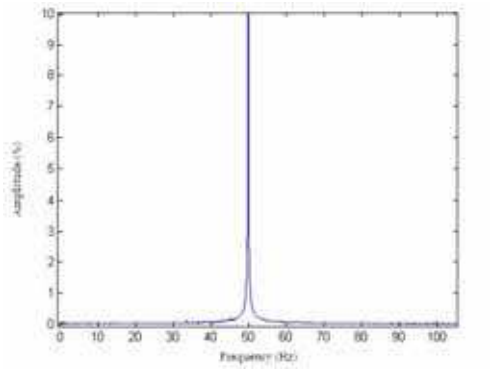

Fig. 21. Normalized FFT of the sampled signal

A nominal rotation speed near to 1000 rpm was assumed (synchronous motor speed). Knowing the nominal power of the engine, it can be deduced from the current consumption during the test that speed will be very close to that of synchronism.

From this hypothesis, we took a speed window from 970 rpm to 997 rpm to estimate the eccentricity frequency. For these speed values the eccentricity associated frequency corresponds to 33.83 Hz and 33.38 Hz. In Fig. 22 is possible to distinguish a peak on the 33.4 Hz.

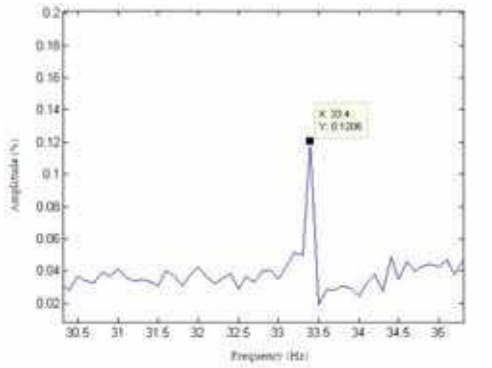

Fig. 22. f_{exc} determination

By calculating the exact associated eccentricity frequency from a_k and a_{k+1} harmonics, it is possible to determine that the engine speed is n_r = 994rpm, which is consistent with the previously known facts of the engine tested. In Figures 23, 24 25 y 26 the failure associated frequency is shown for each of the tested failure (broken bars, short-circuit, bearing damage and eccentricity).

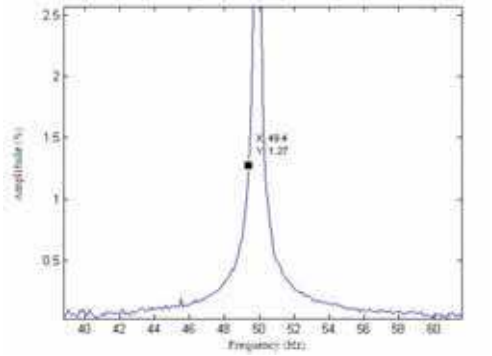

Fig. 23. Broken bars associated frequency

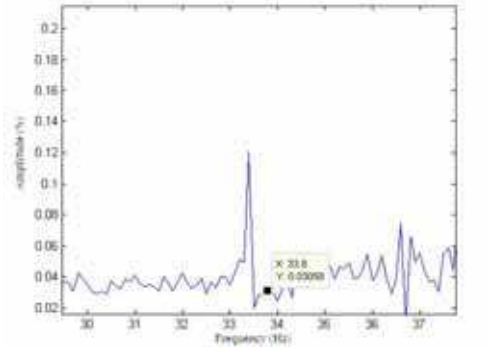

Fig. 24. Short-circuit associated frequency

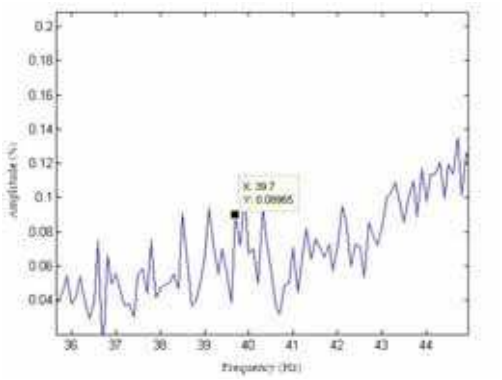

Fig. 25. Bearing damage associated frequency

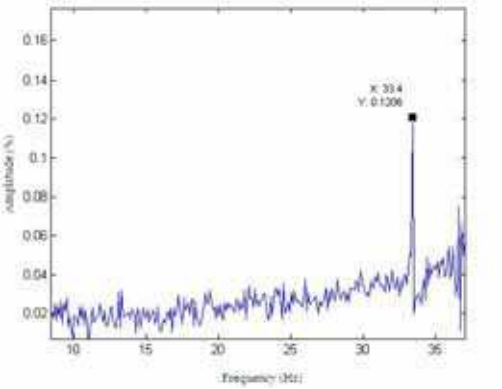

Fig. 26. Eccentricity associated frequency

From the figures presented above, it is possible to infer that the condition of the engine tested for defects studied is good. The only fault is raised above the standard is for broken bars, but this behavior is expected due to the proximity of the engine speed with its synchronous speed.

5. Summary and conclusions

The main objective of this work has been to determine a monitoring and diagnosis methodology for asynchronous motors which can be applied at the industrial level.

The proposed system is able to ascertain the exact value of the harmonic in study regardless of the sampling time.

This methodology gives encouraging results. It is possible from this technique to determine the exact extent of the defect and the associated frequency. In this way, the study of the growth tendencies of failures is easier. Also a practical slip estimation method for these motors has been introduced. This method requires minimum sensorization and the no need to remove the motor while doing the tests.

Laboratory tests results for broken rotor bars, short-circuit, eccentricities and bearing faults are shown. The method was validated for the failures studied. The results show that it is possible by this method to detect the failures in an incipient stage. Finally the results of industrial tests show the accuracy of the methodology.

6. References

Bellini, A. Filippetti, F. Franceschini, G. Tassoni, C. & Kliman, G. B. (2002); On-field experience with online diagnosis of large induction motors cage failures using MCSA, IEEE Trans. on Ind Applications, Vol. 38, Nº 4, pp. 1045-1053

Botha, M. M (1997). Electrical Machines Failure, Causes and Cures, Electrical Machines and Drives. 8th annual conference of IEEE, Nº 444, pp. 114-117, 1-3 de September of 1997

Thomson, W.T (1999). A Review of On-Line Condition Monitoring Techniques for Three-Phase Squirrel-Cage Induction Motors – Past, Present and Future, The Robert Gordon University, Schoolhill, Aberdeen, Scotland

Thomson, W.T. & Fenger, M. (2001). Current Signature Analysis to Detect Induction Motor Faults, IEEE Ind. Applications Magazine.

Thomson, W.T. & Gilmore, R. J. (2003). Motor Current Signature Analysis to Detect Faults in Induction Motor Drives- Fundamentals, Data Interpretation, and Industrial Case Histories. Proccedings of 32rd Turbomachinery Symposium.

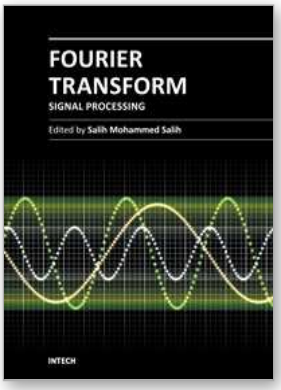

Fourier Transform - Signal Processing
Edited by Dr Salih Salih

ISBN 978-953-51-0453-7
Hard cover, 354 pages
Publisher InTech
Published online 11, April, 2012
Published in print edition April, 2012

The field of signal processing has seen explosive growth during the past decades; almost all textbooks on signal processing have a section devoted to the Fourier transform theory. For this reason, this book focuses on the Fourier transform applications in signal processing techniques. The book chapters are related to DFT, FFT, OFDM, estimation techniques and the image processing techqniques. It is hoped that this book will provide the background, references and the incentive to encourage further research and results in this area as well as provide tools for practical applications. It provides an applications-oriented to signal processing written primarily for electrical engineers, communication engineers, signal processing engineers, mathematicians and graduate students will also find it useful as a reference for their research activities.

InTech Europe
University Campus STeP Ri
Slavka Krautzeka 83/A
51000 Rijeka, Croatia
Phone: +385 (51) 770 447
Fax: +385 (51) 686 166
www.intechopen.com

InTech China
Unit 405, Office Block, Hotel Equatorial Shanghai
No.65, Yan An Road (West), Shanghai, 200040, China
中国上海市延安西路65号上海国际贵都大饭店办公楼405单元
Phone: +86-21-62489820
Fax: +86-21-62489821